

ECRH Superposition on Linear Cylindrical Helicon Plasma in the LMD-U

Kunihiro KAMATAKI, Sanae-I. ITOH, Shigeru INAGAKI, Hiroyuki ARAKAWA¹⁾,
Yoshihiko NAGASHIMA²⁾, Takuma YAMADA²⁾, Masatoshi YAGI, Akihide FUJISAWA
and Kimitaka ITOH³⁾

Research Institute for Applied Mechanics, Kyushu University, Kasuga, Fukuoka 816-8580, Japan

¹⁾*Interdisciplinary Graduate School of Engineering Sciences, Kyushu University,
Kasuga, Fukuoka 816-8580, Japan*

²⁾*Graduate School of Frontier Sciences, The University of Tokyo, Kashiwa, Chiba 277-8561, Japan*

³⁾*National Institute for Fusion Science, Toki, Gifu 509-5292, Japan*

(Received 7 December 2009 / Accepted 13 April 2010)

Electron cyclotron resonance heating (ECRH) is superimposed on a linear cylindrical helicon plasma in the Large Mirror Device-Upgraded (LMD-U) to study the fluctuation characteristics of high density helicon plasma with/without ECRH injection. The radial profiles of electron density and electron temperature rose by $< 10\%$, and the drift wave frequency decreased with the ECRH injection. Bicoherence analysis reveals that the nonlinear interaction between drift waves and broad frequency band components exists with or without ECRH injection.

© 2010 The Japan Society of Plasma Science and Nuclear Fusion Research

Keywords: ECRH superposition, helicon plasma, drift wave, turbulence, linear cylindrical device

DOI: 10.1585/pfr.5.S2046

1. Introduction

Plasma transport across a magnetic field is strongly affected by low-frequency fluctuations, e.g., drift waves, the frequency of which is much lower than the ion cyclotron frequency [1]. Many laboratory linear plasma experiments have been conducted to determine the basic physics of low-frequency fluctuation turbulence, e.g., the drift wave turbulence [2–10]. The nonlinear self-regulation mechanism of drift wave turbulence has been examined to clarify the dynamics of the structural formation of plasma turbulence (refer, e.g., reviews [11, 12]). For a comprehensive understanding of this mechanism, it is important to observe the nonlinear interaction between fluctuations in a wide parameter range in turbulent plasma. Electron cyclotron resonance heating (ECRH) is considered a useful tool for varying the function by controlling T_e in toroidal plasmas. In laboratory linear plasma experiments, helicon waves are usually used to produce high-density, low-temperature plasmas. Despite the effectiveness of ECRH, its impact on fluctuations in linear cylindrical plasma has not yet been reported. In this paper, we superimposed ECRH on helicon plasmas in the Large Mirror Device-Upgraded (LMD-U) [8–10, 13]. The fluctuations are measured to examine turbulence in the plasma. Changes in the fluctuation spectrum and nonlinear interaction among fluctuations were observed in the ECRH-injected plasma.

2. Experimental Setup

At one end of the LMD-U device, a conventional helicon source with a frequency of 7 MHz and rf power of 3 kW is installed for plasma production. The LMD-U plasma source uses a double-loop antenna. The antenna is wound around a quartz tube, 40 cm long with a 10 cm inner diameter. The LMD-U has a vacuum vessel 374 cm long and 45 cm in diameter [Fig. 1 (a)]. At the opposite end of the device, a microwave launcher with a frequency of 2.45 GHz and microwave power of 0.8 kW is installed.

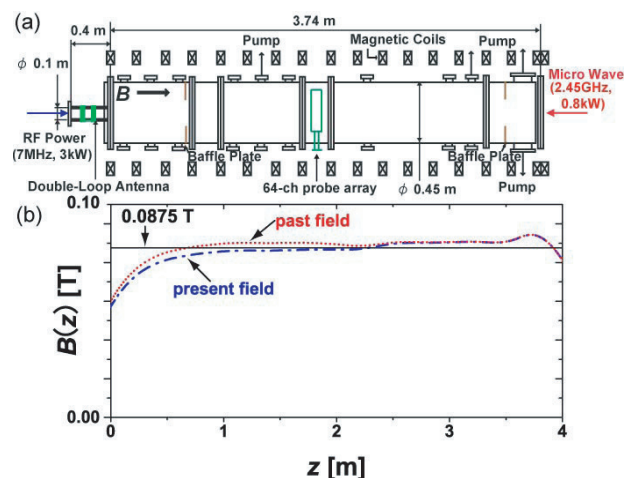


Fig. 1 (a) Schematic view of the LMD-U linear plasma device and (b) axial magnetic field profile.

author's e-mail: kamataki@riam.kyushu-u.ac.jp

Any mismatch of the microwaves is compensated for by using an automatic tuner system. In this study, argon gas is used with a pressure of 2 mTorr. The plasma parameters were measured with a Langmuir probe and a 64-channel probe array [9], which deduce the spectrum $S(m, f)$, where m is the poloidal mode number. The radial profiles of the mean plasma parameters are obtained from the current-voltage (I-V) characteristics of the movable double probe. A magnetic field strength B of up to 0.15 T is generated by the coils around the vacuum vessel. The magnetic field configuration is adjusted so that the resonance layer ($B = 0.0875$ T) is located around the axis position $z = 230$ cm. Here, $z = 0$ shows the position of the boundary between the cylindrical vacuum chamber and the helicon source. The magnetic configuration is different from that used in previous research [8–10, 13] in the LMD-U [Fig. 1 (b)], and thus the plasma features differ from the those previously observed, (e.g., the radial profiles of plasma parameter and the poloidal structure).

3. Experimental Results

A typical time evolution of ion saturation current I_{is} at $r = 4$ cm and $z = 177.5$ cm is shown in Fig. 2 (a). The helicon discharge is sustained for 0.5 s. ECRH is injected from $t = 0.15$ –0.4 s. Figure 2 (b) shows typical auto-power spectra of I_{is} for both the helicon discharge phase ($t = 0.05$ –0.15 s) and ECRH injection phase ($t = 0.15$ –0.4 s). The frequency and poloidal mode number resolutions are 61 Hz and 1, respectively, and the number of ensembles are 200. Figures 2 (c) and (d) show the power spectra $S(m, f)$ with and without ECRH, respectively. Positive (negative) frequency means that the modes propagate in the electron (ion) diamagnetic direction. Here, m means the poloidal number; the frequency resolution is 61 Hz, and the number of ensembles are 30. Multiple peaks appear in these spectra. A peak at $(m, f) = (1, -1$ kHz) is observed with and without ECRH. In the helicon discharge phase, three peaks are located at $(m, f) = (1, 3.1$ kHz), $(3, 5.3$ kHz) and $(2, 6.3$ kHz). In the ECRH injection phase, the peaks are observed at $(m, f) = (1, 2.7$ kHz), $(3, 4.1$ kHz) and $(2, 5.1$ kHz). The frequencies of the $m = 1, 2$, and 3 modes change with ECRH injection. Figures 3 (a)–(c) show the radial profiles of electron density n_e , electron temperature T_e and the floating potential V_f . The maximum n_e increases from 0.9×10^{13} cm $^{-3}$ to 1×10^{13} cm $^{-3}$ and the maximum T_e changes from 2.4 eV to 2.5 eV with ECRH injection. The value of $-\nabla n_e/n_e$ has a maximum at $r = 3$ –4 cm in both phases.

3.1 Mode identification

The main instabilities are $(m, f) = (2, 6.3$ kHz) in the helicon discharge phase and $(m, f) = (2, 5.1$ kHz) in the ECRH injection phase. We call these instabilities H1 and E1. These two observed modes are identified as drift waves by comparison with the general characteristics of

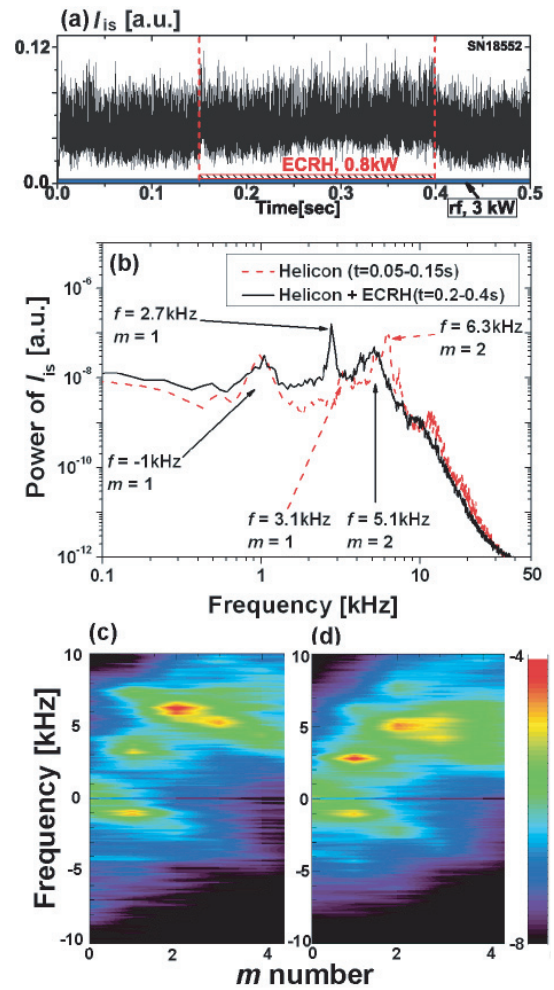


Fig. 2 (a) Time evolution of I_{is} , (b) auto-power spectrum of I_{is} in both phases, and counter-plots of poloidal mode number-frequency spectra $S(m, f)$ in the (c) helicon discharge phase and (d) ECRH injection phase.

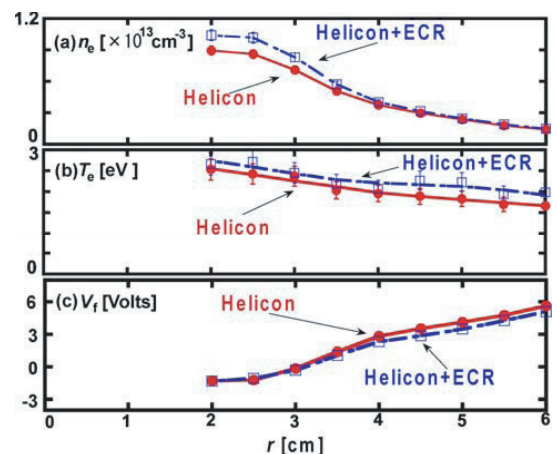


Fig. 3 Radial profiles of (a) electron density n_e , (b) electron temperature T_e and (c) floating potential V_f in the helicon discharge phase (solid line) and the ECRH injection phase (dotted line).

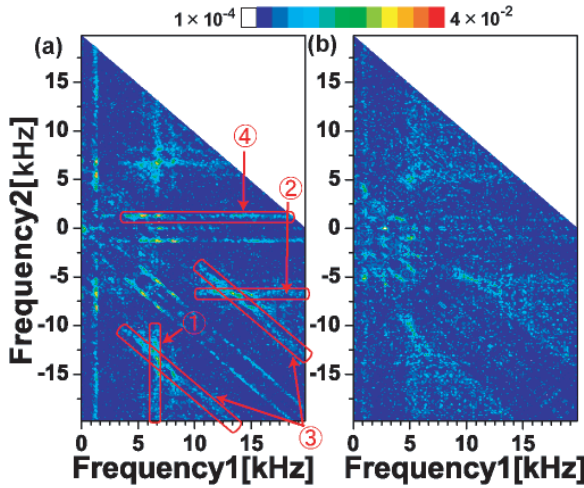


Fig. 4 Squared auto-bicoherence planes of I_{is} calculated using 200 realizations in the (a) helicon discharge and (b) ECRH injection phases. Peaks on red lines indicate each region ① $f_1 \sim 6.3$ kHz, ② $f_2 \sim -6.3$ kHz, ③ $f_1 + f_2 \sim \pm 6.3$ kHz and ④ $f_1 \sim 1$ kHz.

drift waves [14]. The observed experimental characteristics of H1 and E1 are as follows. 1) The normalized amplitudes $|\tilde{\phi}/T_e| \leq |\tilde{n}_e/n_e|$ are at $r = 3-4$ cm. 2) Density fluctuations lead the potential fluctuations by 7° in the helicon discharge phase and 21° in the ECRH injection phase. 3) The poloidal and axial mode numbers are $m = 2$ and $n = 1$ in both phases. Here, the wavelength is the same as the device length. These results show that H1 and E1 have the general characteristics of drift wave instability. If the same analysis for mode identification is applied to other peaks $[(m, f) = (3, 5.3 \text{ kHz})$: H2 in the helicon discharge phase and $(m, f) = (3, 4.1 \text{ kHz})$: E2 in the ECRH injection phase], these peaks also have the general characteristics of drift waves. Thus, these results suggest that the drift wave modes H1 and H2 are transformed to modes E1 and E2 with ECRH injection.

We investigate the nonlinear interaction between drift waves in each phase using bicoherence analysis [15]. Figures 4(a) and (b) show the results of the squared auto-bicoherence of I_{is} . The frequency resolution of the bispectrum is 122 Hz. To optimize the statistics, these squared auto-bicoherences are calculated using 200 ensembles. The graph is symmetric with respect to the line $f_1 = |f_2|$. In the helicon discharge phase [Fig. 4 (a)], peaks are found along the lines ① $f_1 \sim 6.3$ kHz, ② $f_2 \sim -6.3$ kHz, ③ $f_1 + f_2 \sim \pm 6.3$ kHz and ④ $f_1 \sim 1$ kHz. Strong peaks on these lines indicate strong nonlinear interaction between a drift wave at 6.3 kHz and the broad frequency band components at frequencies above 12.6 kHz [shown as lines ① and ② in Fig. 4 (a)]. This suggests that the energy of drift waves and that of the high-frequency components might be mutually exchanged. Similarly, in the ECRH injection phase [Fig. 4 (b)], nonlinear coupling between drift wave ($f = 5.1$ kHz) and broad frequency band components ($f >$

10.2 kHz) occurs. Nonlinear coupling between drift waves and the mode $(m, f) = (1, -1 \text{ kHz})$ occurs in both phases. Although a strong nonlinear interaction between the $(m, f) = (1, -1 \text{ kHz})$ mode and the broad frequency band components ($f > 5$ kHz) in the helicon discharge phase [Fig. 4 (a)] occurs [for example, line ④ in Fig. 4 (a)], the same type of nonlinear coupling weakens in the ECRH injection phase [Fig. 4 (b)]. Summarizing these results, the drift wave interacts directly with broad frequency band components in both phases. However, the mode $(m, f) = (1, -1 \text{ kHz})$ has a different nonlinear coupling with the broad band components in each phase. Differences in these radial profiles are small as shown in Fig. 3, however, some changes in the fluctuation spectrum and bicoherence results are significant. Similar phenomena have appeared in other studies [7]. Thus, a few changes in the radial profiles of plasma parameters might lead to differences in the frequency spectrum and nonlinear interaction among modes.

4. Discussion

4.1 Comparison between observed and numerical results

The observed frequencies of E1 and H1 are significantly smaller than the real drift frequency $f_* = \omega_* / 2\pi = 18$ kHz ($m = 2$) in the helicon discharge phase, and $f_* = 27$ kHz ($m = 2$) in the ECRH injection phase at $r = 3-4$ cm. These frequencies are below the ion cyclotron frequency $f_{ci} = \Omega_{ci} / 2\pi \sim 33$ kHz. As mentioned above, the observed drift frequency ($f = 5-6$ kHz) are significantly smaller than the real drift wave frequency. We consider the cause of this difference. The $\mathbf{E} \times \mathbf{B}$ drift frequency and/or the effect of collision are considered the most likely candidates. The $\mathbf{E} \times \mathbf{B}$ drift frequency is obtained from the radial electric field $E_r (= -\nabla V_s)$. Here, the profile of space potential V_s can be estimated from the equation $V_s = V_f + \alpha T_e$ [16]. The $\mathbf{E} \times \mathbf{B}$ drift ($r \sim 4$ cm) are $f_{E \times B} = (m/r) (v_{E \times B} / 2\pi) \sim 3.7$ kHz (helicon discharge phase) and ~ 4 kHz (ECRH injection phase) ($m = 2$) in the electron diamagnetic direction. The effect of the Doppler shift is smaller than the difference between the observed frequencies and the real drift wave frequency f_* . Next, we calculate the collision drift frequency using the local dispersion relation model (the Hasegawa-Wakatani model [17]), which takes into account the effects of electron collisions and ion-neutral particle collision. The plasma parameters are taken from experimental observations ($m = 2, n = 1, \nu_e / \Omega_{ci} = 250$ and $\nu_{in} / \Omega_{ci} = 0.4$). Here, $\nu_e (= \nu_{ei} + \nu_{en})$, where ν_{ei}, ν_{ei} and ν_{in} indicate the electron collision, electron-ion collision, electron-neutral particle collision and the ion-neutral particle collision frequencies, respectively [18]. The numerical results show that the calculated collision drift wave frequency is close to the observed drift wave frequency ($f = 5-6$ kHz). The $\mathbf{E} \times \mathbf{B}$ drift frequency is not taken into account in this calculation.

Finally, we assume that these differences between the

observed frequencies and the real drift frequency f_* are the result of collisions since the frequency of the collisional drift mode depends strongly on the effects of collisions, ν_{ei} , ν_{en} and ν_{in} which decrease the real drift wave frequency, as shown in Ref. [17].

4.2 Comparison of drift wave frequencies in each phase

Next, we compare the observed drift frequencies in the helicon discharge and ECRH injection phases. The observed drift frequencies decrease from 6.3 kHz to 5.1 kHz ($m = 2$) and 5.3 kHz to 4.1 kHz ($m = 3$) with ECRH injection. The differences between these frequencies is about 1.2 kHz, which cannot be explained by the difference in Doppler shifts between two phases. To confirm this accurately, it is necessary to measure the distributions of neutral particle density and ion temperature (which is related to ν_{in}) experimentally. The fact that the frequency of mode $(m, f) = (1, -1 \text{ kHz})$ remains in both phases, and the identification of another mode $(m, f) = (1, 2.7 \text{ kHz})$ in the ECRH injection phase, are left for future study.

5. Summary

In this study, ECRH is superimposed on a linear cylindrical helicon plasma in the LMD-U to investigate the fluctuation characteristics of a combined ECRH-helicon plasma. ECRH injection changes the auto-power spectrum and the radial profile of plasma parameters; for example, the drift wave amplitudes change, the frequencies decrease, and n_e and T_e increase. The main modes, $(m, f) = (2, 6.3 \text{ kHz})$ in the helicon discharge phase and $(2, 5.1 \text{ kHz})$ in the ECRH injection phase are identified as drift waves by comparing the experimental results and the general characteristics of drift waves. These results suggest that the high collision frequencies ν_e and ν_{in} cause the decrease from the theoretically estimated drift wave frequency to that observed. In addition, bicoherence analysis reveals that nonlinear interaction between the drift waves and the broad frequency band components occurs in both phases. However, a strong nonlinear interaction between the mode $(m, f) = (1, -1 \text{ kHz})$ and the broad fre-

quency band components ($f > 5 \text{ kHz}$) in the helicon discharge phase weakens with the ECRH injection. These findings allow us to investigate experimentally the relevant dynamics, including excitation, saturation, and damping of the fluctuations, which will be reported in future work.

Acknowledgment

This work was partly supported by a Grant-in-Aid for Scientific Research (S) from the Japan Society for the Promotion of Science (JSPS) (21224014), a collaboration program between the RIAM of Kyushu University and the National Institute for Fusion Science (NIFS) (NIFS07KOAP017), and Research Fellowship for Young Scientists from JSPS.

- [1] W. Horton, *Rev. Mod. Phys.* **71**, 735 (1999).
- [2] T. Klinger *et al.*, *Phys. Rev. Lett.* **79**, 3913 (1997).
- [3] C. Schröder *et al.*, *Phys. Plasmas* **12**, 042103 (2005).
- [4] G. R. Tynan *et al.*, *Plasma Phys. Control. Fusion* **48**, S51 (2006).
- [5] M. Ramisch *et al.*, *Plasma Phys. Control. Fusion* **49**, 777 (2007).
- [6] D. C. Pace *et al.*, *Phys. Plasmas* **15**, 122304 (2008).
- [7] K. Kamataki *et al.*, *Plasma Phys. Control. Fusion* **50**, 035011 (2008).
- [8] K. Terasaka *et al.*, *Plasma Fusion Res.* **2**, 031 (2007).
- [9] T. Yamada *et al.*, *Nature Phys.* **4**, 721 (2008).
- [10] Y. Nagashima *et al.*, *J. Plasma Fusion Res. Series* **8**, 50 (2009).
- [11] P. H. Diamond *et al.*, *Plasma Phys. Control. Fusion* **47**, 5 (2005).
- [12] K. Itoh *et al.*, *Transport and Structural Formation in Plasmas* (Bristol and Philadelphia: Institute of Physics Publishing, 1999).
- [13] H. Arakawa *et al.*, *Plasma Phys. Control. Fusion* **51**, 085001 (2009).
- [14] D. L. Jassby, *Phys. Fluids* **15**, 1590 (1972).
- [15] Y. C. Kim *et al.*, *IEEE Trans. Plasma Sci.* **RS-7**, 120 (1979).
- [16] I. H. Hutchinson, *Principle of Plasma Diagnostics* (Cambridge University Press, Cambridge, 2002) 2nd ed.
- [17] K. Kamataki *et al.*, *J. Phys. Soc. Jpn.* **76**, 054501 (2007).
- [18] M. A. Lieberman *et al.*, *Principles of Plasma Discharges and Material Processing* (Wiley, New York, 1).